Fracture Mechanics of Concrete and Concrete Structures -
Assessment, Durability, Monitoring and Retrofitting of Concrete Structures- B. H. Oh, et al. (eds)

Cementitious composites during leaching and drying: X-ray microtomography analysis of cracking pattern dependence on size of rigid inclusions

C. Peng, T. Rougelot, N. Burlion
Laboratoire de Mécanique de Lille, UMR CNRS 8107, Polytech'Lille, Villeneuve d'Ascq, France

D. Bernard
Institut de Chimie de la Matière Condensée de Bordeaux, UPR 9048, Pessac, France

ABSTRACT: Short and long-term behaviors of concrete structures are of importance when dealing with durability aspects. One particular interesting aspect is the change in microstructure of concrete submitted to drying or leaching processes, and a potentially induced cracking pattern. Experimental investigations which focus on the effect of the dimensions of aggregates over cracks are proposed in this paper. The study is conducted on geometrically simplified cementitious materials (composites cementitious matrix-spherical rigid glass inclusions). The samples are submitted to accelerated leaching or to drying, and the evolution of their microstructure is regularly recorded by means of X-ray microtomography, at a resolution of 5.3 µm. Two methods are proposed to study the cracking pattern, which appears to be greatly dependant of the size of inclusions. In particular, it appears that a larger diameter of inclusions tends to increase the crack opening but to decrease the number of distinct cracks.

1 INTRODUCTION

One of the major topic that involves a refined study concerning durability of concrete, and notably its behavior in a short-term (some years) or a long-term (several thousands of years) point of view, is the problematic of deep underground storage of radioactive waste. Indeed, as designed by ANDRA (French Agency for Nuclear Wastes Management) for underground storage in France, the disposal widely uses concrete as a structural and as a confinement material. This choice is explained by its durability, relying on low transport properties (permeability, diffusivity), and a conservation of its main mechanical properties in respect with time, when concrete remains sound.

However, in such an underground disposal, concrete is submitted to a large range of thermal, mechanical, chemical and hydric processes that can be moreover coupled. The applied solicitations, in addition, evolve with time, and may lead to a degradation of confinement properties of concrete or mechanical decrease in strength or delayed strains and displacement by, for instance, a development of a network of cracks.

The chemical and physical mechanisms involved are numerous and with quite different kinetics. The focus can be put on two main mechanisms: drying and leaching. Drying is what a concrete can experience once it has been setup and under various relative humidities and temperatures. This is a rather "short-term" mechanism, as each concrete construction will be early submitted to environmental RH conditions hardly different from its internal water saturation, leading to differential shrinkage between inside and outside part of the structure, and thus to a cracking pattern. These consequences are therefore expected quite quickly, regarding to the designed service-life duration of the structure.

On the contrary, leaching can be considered as a rather "long-term" degradation: it is the result of an attack of a fluid flow inside the porous network (pure water, water with very low pH) which can dissolve some constituents of the cementitious matrix, and mainly calcium Ca. As a result of this decalcification, a modification of the microstructure of concrete can appear, by chemical rearrangement of C-S-H that have been decalcified (Chen et al. 2006). Differential shrinkage linked to this rearrangement between sound and leached parts also can lead to a cracking network, as was yet shown in previous work (Rougelot et al. 2009).

A careful study of the evolution of the microstructure and of the cracking network under such degradation mechanisms is essential. X-Ray microtomography has proved to be an adequate technique to highlight at such a scale these phenomena, to qualitatively characterize them. Some authors have yet proposed some techniques to quantify these evolutions of porous network observed by X-ray microtomography, mainly for cementitious materials submitted to compression (Landis & Nagy 2000) or change in tortuosity during hardening by means of random walk simulation (Promentilla et al. 2009).

In this paper, experimental investigations of effect of drying and leaching over cracking are proposed. The geometrical complexity of concrete and usual aggregates is a problem when aiming at quantifying changes in this microstructure (difficulties in good segmentation of voids from "solid" part and in good understanding of physical mechanisms). The study is conducted on geometrically simplified cementitious materials made of cement pastes and glass spheres. The investigations are performed on composites with various inclusions diameters (1, 2 and 4 mm) to check the effect of aggregate diameter over the cracking pattern.

Obtained microtomographic data have therefore to be exploited to get quantitative values. Time and technical competences to perform this analysis is impressive, due to material complexity and difficulties in setting up an automated reliable protocol. Thus, this paper explores two techniques which aim at quantifying changes in microstructure, notably for drying specimens: a rather "rough" one whose goal is to propose a fast way to get comparative quantitative results, even if associated imprecision can remain quite high, and a very refined one, to validate the previously obtained "rough" results.

2 EXPERIMENTAL SETUP

This paragraph sums up the main characteristics of the experimental setup used to get X-ray microtomographic data of cementitious composites under drying or leaching.

2.1 *Materials choice*

The chosen material consists of a cementitious composite initially proposed by (Bisschop & van Mier 2002) made of a cementitious matrix with rigid glass spheres. This "simplified" material allows a better analyze of physical and mechanical phenomena during leaching and drying, by simplifying the geometrics of the microstructure.

The matrix is composed of cement paste with a water-to-cement ratio of 0.5 (cement CEM II/B 32.5 R). The volume fraction of glass spheres (which act as aggregates) is 35% for all tested composites. The choice of glass spheres is explained by the similitude of mechanical properties with those of real siliceous aggregates.

The use of microtomographic imaging limits the dimensions of the sample. Therefore, the diameters tested for the spheres are 1, 2 or 4 mm. The composites will be called C1 for composites with glass inclusions of 1 mm, C2 with 2 mm and C4 for 4 mm. The specimens are cylindrical cores (8 mm diameter, height: about 20 to 30 mm) taken from prismatic beams 40*40*160 mm cured for 28 days in a lime-saturated water (20°C), and then protected from desiccation with sheets of aluminium. It is assumed that for 1 and 2 mm composites (C1 and C2), the specimens are representative of the material (diameter of the specimen is at least four times larger than aggregates), whereas for 4 mm spheres (C4), they have to be considered as only indicative. All results for all diameters will not be presented in this paper.

2.2 *Microtomographic acquisition*

The microtomographic acquisition was performed on beamline BM05 of the ESRF (European Synchrotron Radiation Facility) in France, with a FRELON CCD camera of 2,048x2,048 pixels. The resolution was of 5.3 µm, hence the scanning zone is about 10 mm high. This set of projections allows to reconstruct a three dimensional map of X-ray attenuation coefficient, which is essentially linked to material density. The value of this attenuation coefficient is coded on 8 bits (values from 0 to 255) and is represented by an associated gray level. Hence, it is possible to clearly see the different constituents of the cementitious composites (cement paste, voids, cracks, leached zone…). The acquisition of one sample is achieved by scanning the top part of the cylindrical specimen, then the bottom part but with an overlapping zone with the top part, to facilitate the global reconstruction of one sample.

2.3 *Drying and leaching processes*

Specimens are scanned by X-ray microtomography when they are sound, and this constitutes the reference state of the specimen.

The samples submitted to drying are placed in an oven, and follow those successive steps:

- 30 hours at 60°C
- 20 hours et 105°C
- 22 hours at 150°C

A microtomographic acquisition is realized after 24, 48 and then 72 hours of drying.

For the accelerated decalcification process (Carde et al. 1997), samples are immerged in an ammonium nitrate solution (NH_4NO_3, concentration: 480g / kg_{H2O}) and regularly scanned, as shown in Figure 1.

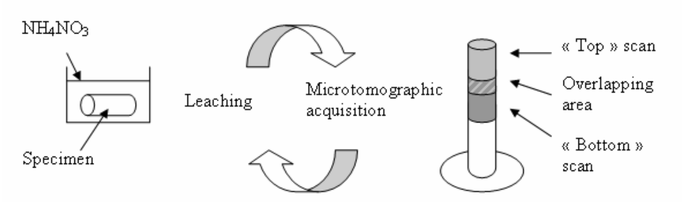

Figure 1. Principle of microtomographic acquisition of samples submitted to leaching.

3 RAW EXPERIMENTAL DATA AND "ROUGH" ANALYSIS

From the reconstructed 3D images of samples in sound or degraded states, slices can be extracted in any part of the specimen. Some examples are presented below, to highlight changes in the microstructure, and the different behavior depending on the glass sphere diameter, mainly concerning the cracking pattern.

3.1 *Dried specimens: microtomographic data*

The figures 2 and 3 present a slice of a 3D reconstruction of a specimen dried during 48 hours with spheres of 2 mm (Fig. 2) and 4 mm (Fig. 3).

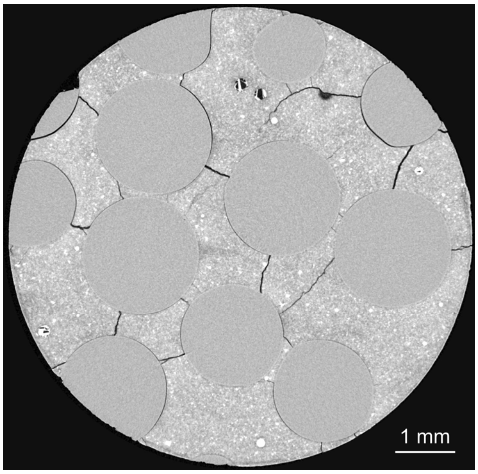

Figure 2. Microtomographic slice of a composite C2 after 48 hours of drying.

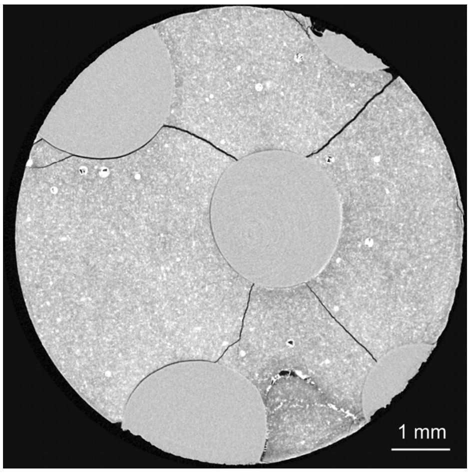

Figure 3. Microtomographic slice of a composite C4 after 48 hours of drying.

Whereas the sound state of those composites C2 and C4, before drying, was not exhibiting any cracks, a cracking pattern linked to drying shrinkage is clearly shown on these slices. Moreover, it clearly appears a change in the cracking pattern in relation with the diameter of the glass aggregates. The composite C2 has more numerous cracks, which link inclusions, than for the composite C4. However, the total volume of cracks seems to be about the same for C2 and C4, thus indicating that both length and crack opening should be smaller in the C2. This is partly verified on figure 3 where opening of the top-right crack appears to be slightly higher than any crack of the C2 on figure 2. As a partial conclusion from these experimental data, increasing the specific area of rigid inclusions (by decreasing the diameter of glass beads) leads to more diffuse cracks, but with a smaller opening. Cracks tend to be more opened when the number of inclusions is limited.

3.2 *Rough analysis of dried specimens*

A심부름 first step rough image analysis can be performed to try to validate the experimental observations of the above paragraph, by quantifying evolution of cracks with drying. On these sections, a threshold filter is applied to convert the 8-bit image into a binary one. The goal is to make a distinction between solid phase and voids. Thus the attenuation coefficient coded by a value varying between 0 and 255 (in 8-bit image) is changed in a binary attenuation value: each voxel whose gray level is under the threshold is considered as black voxel (binary value: 1) and stands for "void". On the contrary, other voxels have a binary value of 0. The figure 4 shows the binary image of the slice of C2 represented in figure 2. Then the number of black pixels inside the specimen is calculated. To avoid some problems with the edge of the specimen, a rectangular region of interest of 900*1000 pixels is studied, and its location is indicated in Figure 4.

However, the location of the studied slices is about the same at each step of drying for a given composite, and may distort the calculated value of black pixels, which take into account both air bubbles, initial porosity and cracks. Indeed, air bubbles have an "area" on slices that can be higher than the area attributed to cracks. This may lead, if the studied slice is not exactly the same between two successive steps of drying, to a change in the diameter of air bubble and a great modification of number of black pixels that cannot be attributed to only change in crack number, length and opening.

Therefore, a more representative procedure is proposed. The calculation of number of black pixels is performed not on 1 slice but on 3 sets of 100 slices extracted from 3D reconstructed data for each composite, ensuring a better representativity of the crack evolution, and a better comparison between C2 and C4. It has to be noted that each 3D image of a specimen is compound of about 1250 slices, that is to say that one-fourth of the specimen is studied in these calculations.

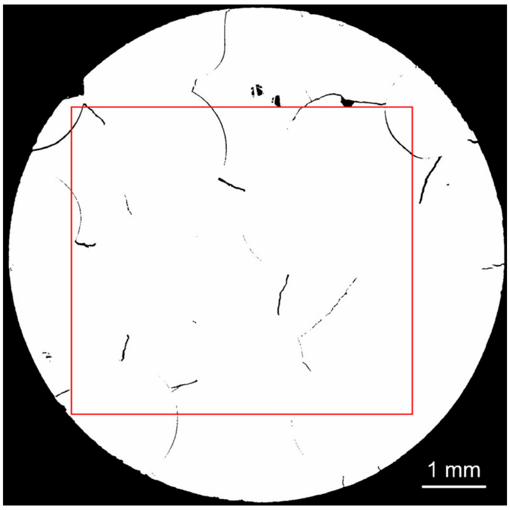

Figure 4. Binary image of the slice of the composite C2 presented in figure2. The rectangle defines the location of the region where black pixels are taken into account.

The following table (Table 1) sums up the calculated value of black pixels for sound, 24h-dried and 48h-dried (and 72 hours for C4) composites C2 and C4, and the absolute evolution between two successive steps of drying. The given values are the mean value measured on the 300 different slices for each composite in a given drying state.

Table 1. Mean number of black pixels and evolution during drying for composites C2 and C4.

	2 mm		4 mm	
Drying time	Number of black pixels	Evolution	Number of black pixels	Evolution
0 hour	2043	-	1237	-
24 hours	4435	2392	4479	3242
48 hours	11022	6587	9895	5416
72 hours	-	-	17015	7120

It is assumed that the evolution in black pixel number, for dried specimen, is only due to crack apparition, as the drying will only lead to cracks inside the cementitious matrix, and not increase of the initial porosity.

The table 1 indicates that indeed, the crack volume seems to be quite equivalent for C2 and C4, provided that initial porosity and air bubble volumes was higher for C2 on the studied slices. Moreover, the evolution in crack volume is about the same, with an increase of 2392 pixels for C2, then 6587, whereas this evolution is of 3242 and 5416 for C4. The small differences can probably be attributed to the approximations done, notably by only selecting a rectangular section inside the specimen and by the fact that the location of slices is not perfectly identical (images have not been registered). Therefore, it appears that this first analysis is a rather good first step at quantifying crack evolution, but it is necessary to more deeply analyze those microtomographic data to check if the drawn conclusions can be confirmed, by extracting reliable data. This will be dealt with in §4.

3.3 *Leached specimens*

As previously done for dying samples, specimens after different times of leaching are observed by means of microtomography.

To perform the same kind of quantification of cracking evolution than for drying samples, the first step is again to convert the slices into binary images (with a threshold filter). The figures 5 and 6 show binary slices hence obtained for a 1 mm and 2 mm composites decalcified in ammonium nitrate solution for 120 hours.

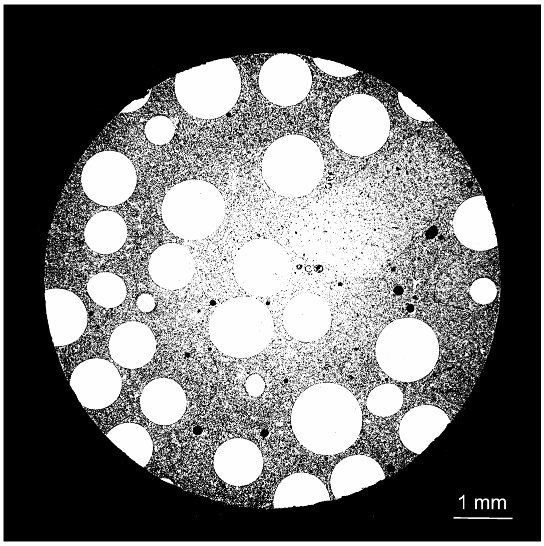

Figure 5. Binary image of a composite C1 after 120 hours of leaching.

After this time of degradation, portlandite has been totally removed and C-S-H are being decalcified. As it can be clearly seen, the cracking pattern between composites C1 and C2, due to decalcification shrinkage, is greatly different. For 1 mm composites, only some small cracks are larger than the microtomographic resolution and are visible (opening about 1 pixel, i.e. 5.3 µm). The visible cracks are more important with 2 mm glass sphere composites. Cracks appear wider, openings varying between 1 and 3 pixels. A same conclusion can be drawn by comparing 1 mm (not presented in this paper) and 2 mm composites submitted to drying. Hence, the dependence of the cracking pattern to the inclusion diameter is well underlined. The crack opening in C1 is lower than in C2. The increasing number of inclusions (and as a consequence specific area of glass inclusions) for a given fraction volume ratio (35%) inside the composite tends to decrease the width and length of cracks.

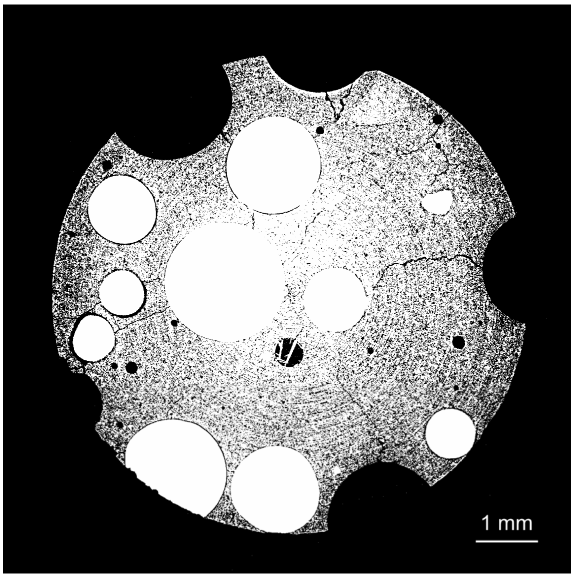

Figure 6. Binary image of the composite C2 after 120 hours of leaching.

If a rough quantification of this crack dependence to inclusion diameter want to be performed, some additional issues than those noted for dying composites arise. On the contrary of the analysis of dried specimens, the evolution in black pixels take into consideration cracking but also decalcification of the cementitious matrix, leading to a more porous material. A separation between increase in porosity and in cracks is not easy to achieve, and some future developments are still needed.

4 QUANTIFICATION OF MICROSTRUCTURE EVOLUTIONS

The raw experimental slices presented in the previous paragraph, for a human eye, are relatively quite contrasted and the detection of cracks, glass spheres and leaching front remains a priori easy. Nevertheless, quantification requires being able to measure for example, the crack opening, the volume of cracks, and the evolution during drying or leaching, in a reliable way. The rough analysis proposed in §3 can only extract volume of "voids", but approximations done could lead to some issues in the exploitation of microtomographic results. A more precise analysis is thus needed.

This four-dimensional analysis implies to try to automate the process of segmentation of "voids", and more precisely of cracks, from solid phases. Moreover, 3D images of one sample at different degradation steps need to be registrated to allow exact comparisons of cracking pattern, and to determine its evolution.

From a numerical point of view, 3D microtomographic data of one sample is a file containing for each voxel (extension of the definition of "pixel" in three dimension), whose size is 5.3*5.3*5.3 µm3, an 8-bit value (grey level) accounting for the attenuation coefficient of the constituent of the voxel.

However, some problems arise from this analysis. Even if images seem to be well contrasted, the automated segmentation is actually hard, since for instance the grey level variations of voxels inside a glass sphere is about the same than in the sound part of the cement paste. Reliable determination of the contour of those spheres thus remains quite difficult. As a consequence, image registration only based on spheres which are supposed not to be degraded by both leaching and drying is not possible. In addition, acquisition noise and artifacts can lead to voxel erroneous grey level that should be corrected through different filters and procedures, to be able to extract, in an automated way, cracks from solid paste.

Finally, for samples submitted to decalcification, another issues come. The evolution of "voids" in drying materials is mainly attributed to crack growing whereas for leaching, either calcium depletion or crack apparition modifies the total "void" of the composite. Hence, dealing with cracks in decalcified materials is one degree more difficult as yet statedd. The fact that cement paste attenuation decreases with leaching (by loss of calcium and thus density) is an additional issue, in comparison with drying where the cement paste has the same density at each step (only some cracks will break the continuous matrix).

In the following paragraphs, a technique to deal with crack evolution as a function of aggregate diameter is proposed. For drying, relatively simpler, a semi-automatic procedure is explained. Volume and surface of porosities and cracks are extracted and compared for glass sphere diameter of 2 and 4 mm for several steps of degradation.

4.1 *Refined analysis of dried specimens: pre-filtering*

Before cracking pattern evolution can be quantified, as explained before, some image treatments have to be applied to perform a reliable analysis of the samples. The successive stages used are developed below.

In a numeric image, artifacts stand for each artificial phenomenon, partly independent of the studied material, whose lead to an erroneous recorded intensity (i.e. grey level). Two main artifacts are regularly observed in high-resolution microtomography: hot spot and ring artifact. Their correction is usually quite hard, and must reduce noise without changing the morphology of present structures.

As the procedure wants to be (quasi-)automated to be able to treat a great quantity of data, prefiltering is applied on 2D radiographs, rather than in 3D reconstructed volumes where corrections are generally manual.

Hot spots are due to high energy photons which directly impact the CCD captor, leading to a very local intensity peak. They are treated through a non linear filter called median filter. The key idea of this

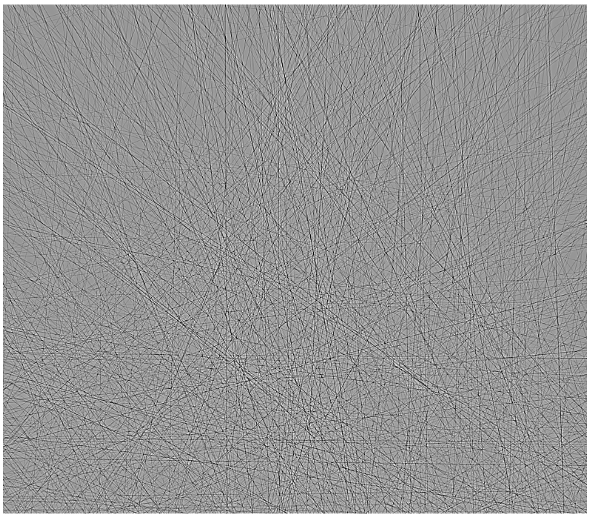

Figure 7. Differential image on a section before and after treatment.

filter is to replace each pixel intensity value which is too far from the median value of the surrounding pixels. The Figure 7 presents the differences between the same sections before and after correction of hotspots.

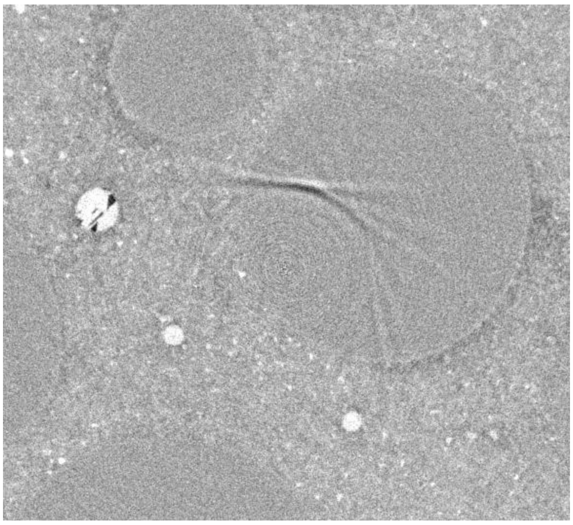

Figure 8. Example of a ring artifact on a slice.

Ring artifacts are another artifact which can be filtered by a Savitzky-Golay filter (fourth order).. The filter is designed to not modify the contours of samples, and to be applied only where it is necessary. Partial rings can also be corrected. The figures 8 and 9 show a zoom on the section where there are ring artifacts without treatment (figure 8) and with filter (figure 9). The made corrections are allow to get a 3D reconstructed image closer of the actual sample.

4.2 *Image registration*

Once the prefiltering process applied, the filtered backprojection algorithm (Natterer 1999) allows to reconstruct the sample with artifacts eliminated. The objective is now to be able to register image. This procedure consists in determining the spatial transformation between two images to match equivalent

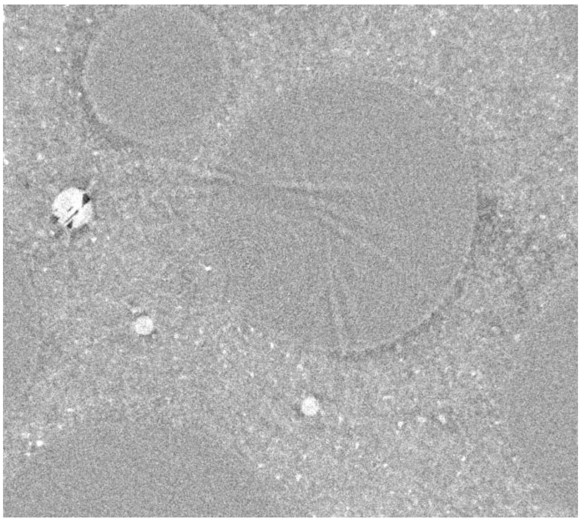

Figure 9. Corrected slice with Savitzky-Golay filter.

characteristics. In the present case, when successive microtomographic acquisitions are performed on a same sample, its position could slightly vary. Therefore, it is not possible to directly compare two 3D images at different steps of degradation without registration in a reliable way. (Noblet 2006) has drawn in his Ph.D thesis a thoroughly review of techniques of registration. Three main points characterize the registration (Jannin et al. 2001):

- attributes: remarkable points of the images, which help guiding registration
- similarity criterion: calculation of differences between attributes to compare them
- transformation model: mathematical function allowing to transform (generally a rigid transformation by rotation and translation is used) one volume in the same reference than another one

The choice of attributes can be achieved manually or automatically. Manually, some defects inside the glass spheres (micro air voids) can be used as attributes since they are considered as “constant” (not degraded by drying or leaching). Same defects are referenced in the referential volume and the volume to be registered. Then, the transformation matrix is calculated to match these points in both volumes. However, this manual choice of attributes is time consuming, as slices of the volumes (referential and to be registered) must be studied to find them.

An automatic method has been developed, and is based on volumes of voxels where attenuation coefficient is very high (anhydrous cement, portlandite). Too small (noise dependant) or large volumes are eliminated. The centers of gravity of these volumes are calculated. Several tens of thousands points are in this manner selected. Then similar points in the referential and to be registered volumes have to be detected. Comparisons are drawn by matching nearby points with an identical volume. Once done, the transformation matrix can be calculated, and registration is complete.

4.3 *Characterization of porosity and cracks*

To analyse the evolution of the sample microstructure during drying, 3D registered images contains too many information. Some representative properties have to be extracted, and have to characterize the evolution of voids, and mainly of cracks. Image analysis gives quantitative data, taking into consideration the shape, the structure and the connectivity of the constituents, and in our study, of voids. This is achieved in this paper by using functions of Minkowski (Blasquez & Poiraudeau 2003). They are initially defined for convex objects, and can account for the volume, the surface, the average length and the connectivity of the voids inside a volume.

As in the rough analysis of dried specimen, the first step is to convert 8-bit images into binary ones, to distinguish solid phase from "voids". A threshold filter is then applied. Each voxel can be seen as an interior, several open facets, open edges and open apexes. In a given volume, the number of black voxels can be calculated, and is noted n3. The number of open facets is called n2, of open edges n1 and of open apexes n0. The four functions of Minkowski are calculated as follows (Equations 1):

$$V = n_3$$
$$S = -6n_3 + 2n_2$$
$$2B = 3n_3 - 2n_2 + n_1$$
$$\chi = -n_3 + n_2 - n_1 + n_0 \qquad (1)$$

where V is the volume of black voxels, S the surface, 2B the average length and χ describing an aspect of an object of the topologic space (also called Euler-Poincaré characteristic).

4.4 *Effect of aggregate diameter on cracking*

The procedure of image analysis is applied to composites with glass spheres of 2 and 4 mm (C2 and C4), as in the §3. The calculations of the functions of Minkowski are performed only on small volumes of interest of the global samples (dimensions 300*300*300 voxels). Only the medium section is represented in these figures. Hence 150 slices above and below this section are taken into consideration in calculations.

In the "rough" analysis of the §3.2, the set of studied slices where not registered. In the present analysis, the calculations on black pixels are a priorimore reliable, and some other data can be extracted through functions of Minkowski.

The results extracted here focus on the volume V of voids and the surface Sof these voids. The evolution of V is presented for composites C2 and C4 for the sound state, and after 24, 48 and 72 hours of drying.

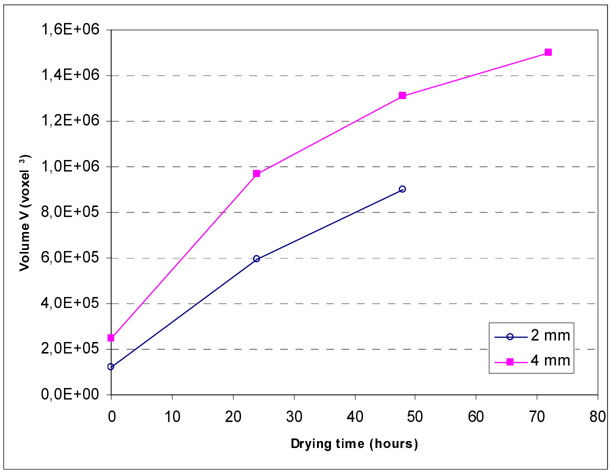

Figure 10. Evolution of volume of voids with time of drying for C2 and C4.

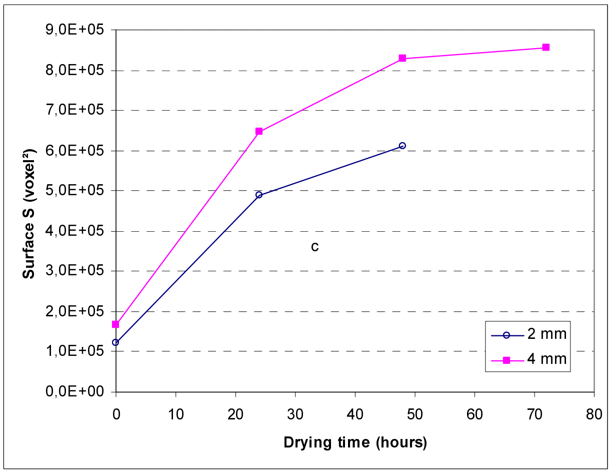

Figure 11. Evolution of surface of voids with time of drying for C2 and C4.

The number of voxels accounting for voids is higher for C4 than for C2. Hence, even if the quantity of initial voids is different (0.123 vs 0.247 million of voxel) and can be attributed to different initial porosity, the number of voxels increases more for C4 than for C2 (difference in voids after 48 hours of drying is about 0,4 million of voxels). The evolution of V between 24 and 48 hours of drying is identical (around 150,000 voxels in addition) for both C2 and C4. However between 0 and 24 hours, the crack increase in volume is more important for C4, thus indicating that cracking pattern is likely to be more dependent to inclusion diameter at the beginning of drying.

The results obtained from this accurate image analysis are slightly different from those obtained in §3.2, where the slope of increase in number of black pixels is higher and higher with time of drying, on the contrary of what can be seen in Figure 10. This could be attributed to the fact that calculation are performed on unregistered images (i.e the location of studied slices in §3.2 are approximatively the same). In addition, the surface of the region of interest has changed, and is more local in the present analysis. This area was selected because of the presence of one air bubble and an initial crack, and this special location may influence the observed behaviour.

Since the difficult work of image registration has been performed for the accurate procedure, the rough analysis of §3.2 can now be performed on registered images, to check if previous conclusions remain the same. For this purpose, only composite C2 is studied under drying. The table 2 sums up the mean values of evolution in the number of black pixels on unregistered (same values than in table 1) or registered images, allowing to estimate the validity of the rough approach.

Table 2. Evolution in number of black pixels for the composite C2. ("rough" analysis performed on unregistered or registered images).

Years	Unregistered images	Registered images
0 to 24 hours of drying	2392	1752
24 to 48 hours of drying	6587	6806

It clearly appears that the trends are similar, thus indicating that the rough analysis on unregistered images implies only small variations in the results, at least in a comparative study. The differences in the slope evolution noticed previously are, as a consequence, mainly due to the choice of the region of interest. Further developments are therefore needed, to perform the accurate analysis on other regions, to limit this local effect on calculations through functions of Minkowski.

The Figure 11 presents the evolution of the surface of voids, thanks to functions of Minkowski, what cannot be achieved in the rough analysis. It can be underlined that the evolution of volume of cracks continues to increase after 48 hours of leaching for C4, whereas the surface of voids tends to an asymptotic value. This could be linked to the fact that all cracks have appeared after 48 hours of drying in the composite C4, and the further drying only increases the crack opening (no new "fresh" crack surface but volume still increases). The tendency appears to be quite similar for C2, with a drastic decrease of the slope after 24 hours of drying, even if no data were accessible after 48 hours.

As a consequence, since there are more numerous cracks in composite C2 for a lower volume of voids, as each inclusion acts as a point of nucleation of cracks, the crack length and opening of C4 is expected to be higher. This image analysis allows confirming the observed tendency done on microtomographic raw slices.

5 CONCLUSIONS

This present study has shown that the cracking pattern of composites cement-glass spheres depends on the diameter of inclusions, when these materials are submitted to drying or leaching. Two main image analysis have been performed, a rather rough one and a more precise one. Both techniques have confirmed the experimental observations done on microtomographic slices. Indeed, the volume of cracks being at least the same, or higher for the composite C4, and since number of cracks are higher for the composite C2, it can be stated that the opening of cracks and length will be different in these two materials. Moreover, by comparing composites C1 and C2 submitted to leaching, this fact that crack opening is smaller when diameter of inclusion is lower (at a given volume fraction) tends to be validated.

These results are of interest in the modeling of hydromechanical behaviour of cementitious materials, by taking into account for instance, the link between the damage variable and the diameter of aggregates at a mesoscopic level.

Future work is nevertheless needed, mainly by developing the current image analysis in order to study the samples submitted to leaching, and by following the exploitation of microtomographic data on composites with other diameters (notably 1 and 6 mm).

REFERENCES

Bisschop, J. van Mier, J.G.M. 2002. Effect of aggregates on drying shrinkage microcracking in cement-based composites. *Mat. Struct.* 35: 453-461

Blasquez, I. Poiraudeau, J. F. 2003. Efficient processing of Minkowski functionals on a 3D binary image using binary decision diagrams. *Journal of WSCG* 11(1).

Carde, C. Escadeillas, G. Francois, R. 1997. Use of ammonium nitrate solution to simulate and accelerate the leaching of cement paste due to deionized water. *Mag. Con. Res.* 49: 295-301

Chen, J.J., Thomas, J.J. Jennings, H.M. 2006. Decalcification shrinkage of cement paste. *Cem. Con. Res.* 36: 801-809

Jannin, P. Grova, C. Gibaud, B. 2001. Fusion de données en imagerie médicale: revue méthodologique basée sur le contexte clinique, *ITBM-RBM* 22 (4) : 196-215, in French.

Landis, E. N., Nagy, E. N. 2000. Three-dimensional work of fracture for mortar in compression. *Engineering Fracture Mechanics* 65: 223-234.

Natterer, F. 1999. Numerical methods in tomography. *Acta Numerica 8:* 107-141.

Noblet, V. 2006. Recalage non rigide d'images cérébrales 3D avec contrainte de conservation de la topologie, Ph D. thesis of University of Strasbourg I, in French.

Promentilla, M.A.B. Sugiyama, T. Hitomi, T. Takeda, N. 2009. Quantification of tortuosity in hardened cement pastes using synchrotron-based X-ray computed microtomography. *Cement and Concrete Research* 39(6): 548-557.

Rougelot, T. Burlion, N. Bernard, D. Skoczylas, F. 2009. About microcracking due to leaching in cementitious composites: X-ray microtomography description and numerical approach. *Cement and Concrete Research*, in press.